Detection of Internal Short Circuit for Lithium-ion Battery Using Convolutional Neural Networks with Data Pre-processing

Minhwan Seo[1], Teadong Goh[2], Minjun Park[1], and Sang Woo Kim[1]
[1] Department of Electrical Engineering, Pohang University of Science and Technology (POSTECH), 77 Cheongam-Ro, Nam-Gu, Pohang, 37673, Korea
[2] Department of Creative-IT Engineering, Pohang University of Science and Technology (POSTECH), 77 Cheongam-Ro, Nam-Gu, Pohang, 37673, Korea
Email: {mhseo09, ehd1116, parkmj, swkim}@postech.edu

***Abstract*—Internal Short Circuit (ISCr) is main cause of dangerous incidents such as thermal runaway in a lithium-ion battery. However, if constant currents are applied to the battery as a load current, existing model-based methods have difficulty in estimating parameters in an equivalent circuit model of the battery accurately, resulting in problem of detection of the ISCr. In this paper, we propose a method for detecting the ISCr in the lithium-ion battery using the Convolutional Neural Networks (CNN). Data pre-processing is conducted to enlarge the effect of ISCr in terminal voltages of the battery, and then the CNN algorithm is used to classify the degree of the ISCr faults. Dataset for the CNN is obtained from a MATLAB/Simulink battery model. The proposed method shows classification result with high accuracy of 96.0% and consequently contributes to detecting the ISCr in the battery early.**

***Index Terms*—internal short circuit, early detection, convolutional neural networks, data pre-processing, lithium-ion battery**

I. Introduction

Demand of lithium-ion batteries for the electric vehicle [1] and the grid system [2] exceeds our expectation recent years due to their high power density and a long cycle life [3]. However, the safety problem about the lithium-ion batteries is still of concern, because of hazardous incidents such as battery failures of both the Boeing 787-7 [4] and the Samsung Note7 [5]. Internal Short Circuit (ISCr) in the battery is main cause of these incidents, and thermal runaway with fire and explosion may be caused by the ISCr when magnitude of ISCr resistance (R_{ISCr}) is lower or equal to 0.27 Ω [6]. Thus, the soft ISCr which has a large magnitude of R_{ISCr} must be detected to prevent the thermal runaway.

Recently, studies for detecting the ISCr in the battery have been introduced [7]-[10]. Thresholds, such as decrease in terminal voltage and increment in temperature caused by the ISCr, were obtained to detect the ISCr [7]. However, the thresholds may not be extracted when the batteries with the soft ISCr are used in prior tests of the ISCr faults. Besides the method based on thresholds, methods for detecting the ISCr with an equivalent circuit model of the battery have been suggested [8]-[10]. After estimating parameters in the equivalent circuit model without the R_{ISCr} and the energy balance equation, the variations of the estimated parameters were used to detect the ISCr [8]. But, only one type of current profile was used to verify this method and the variations obtained with other current profiles may not be identical, leading to difficulty in detecting the ISCr. Therefore, the R_{ISCr}, which directly has information about fault degree of the ISCr, was estimated with the equivalent circuit model with the R_{ISCr} to detect the ISCr from two different current profiles [9]. However, the low accuracy of estimated R_{ISCr} was problem of this method. The estimates of R_{ISCr} in the equivalent circuit model of the battery with ISCr were used to obtain self-discharge currents flowing through the R_{ISCr}, and then the model was updated with the self-discharge currents. Then, the next estimated R_{ISCr} became accurate and was used to detect the soft ISCr correctly [10]. These three methods based on the equivalent circuit model have a common constraint condition: the current whose magnitude varies frequently enough to estimate the parameters in the model accurately must be applied to the battery; i.e., if constant current is used as a load current, the parameters such as Open Circuit Voltage (OCV) and internal resistance in the model cannot be estimated accurately, resulting in problem of detection of the ISCr.

For this reason, a method for detecting the ISCr in the lithium-ion battery discharged by the constant current is proposed using the Convolutional Neural Networks (CNN). To obtain classification results with high accuracy, pre-processing is conducted with input data of the CNN. Due to the high magnitudes of constant currents, the self-discharge phenomenon is not observed clearly in terminal voltages of the battery, which are acquired from various soft ISCr faults and constant currents. The effect of the ISCr in the battery is described distinctly in input data of the CNN, because elements related with the constant currents are removed in the data pre-processing. As a result, the diverse soft ISCr faults

Manuscript received November 26, 2018; revised March 22, 2019.

doi: 10.18178/ijeee.7.1.6-11

can be classified accurately enough to represent the fault degree of the ISCr. To verify the proposed method, the equivalent circuit model of the battery with ISCr was configured in MATLAB/Simulink, and then the simulation data of terminal voltages and constant currents were used as the input data for the CNN.

In the remainder of the paper, the dataset from configuration of simulation is introduced in Section 2, the proposed algorithm is explained in Section 3, the results are discussed in Section 4 and the conclusion are presented in Section 5.

II. DATASET

A. Simulation Configuration

To configure the simulation model of the battery with ISCr in MATLAB/Simulink [11], the first-order RC model [12] of the battery was used. The normal battery (INR 18650-20R, 2.0 Ah) was discharged with a current profile of dynamic stress test and then measurement data of terminal voltages and load currents were used to estimate the parameters, needed to compose the simulation model, using the recursive least squares algorithm [13]. In addition, prior tests for obtaining capacity and relationship between OCV and state of charge (SOC) were conducted, and these two data were also utilized in the simulation model.

B. Data Preparation

The constant currents whose magnitude were in between 1.1C and 3C (2.2 A ~ 6 A) were applied to the simulation model with various soft ISCr fault conditions, such as normal, ISCr 50 Ω, ISCr 30 Ω, ISCr 20 Ω, ISCr 10 Ω and ISCr 5 Ω, for obtaining the terminal voltages. When the battery simulator with 100% SOC was discharged with a constant current as the load current, the terminal voltages and the load currents were stored until the voltage reaches 3.222 V (OCV at 0% SOC). After the voltage is lower than 3.222 V, the stored data of terminal voltage and current were defined as 0 to conduct the zero-padding; this process make the same column size of input data (2 × 3,600) for both ISCr fault cases and a normal case, where the first row of input data is the load current and the second row is the terminal voltage. The number of constant currents with different magnitudes was 1,000 and the number of terminal voltages was also 1,000 for each six different cases (a normal case and five ISCr fault cases); the size of input data was 6,000 × 2 × 3,600 used in the CNN. The training data (800 × 2 × 3,600) were extracted randomly from the data (1,000 × 2 × 3,600) for each six different cases, while the remainder of data (200 × 2 × 3,600) were used as the verification data.

A labelling process was necessary for the supervised learning of the CNN model. The input data for the normal case were labelled as class 1, while other input data for the five fault cases were labelled from class 2 to class 6 in accordance with the ISCr fault conditions.

III. METHOD DESCRIPTION

A. Architecture of CNN

As a particular kind of deep neural networks, the CNN algorithm, which consists of both some filter stages to extract features from the input data effectively and a classification stage, is used in image processing [14] and fault diagnosis [15]. The filter stage contains the pooling layer and the convolutional layer denoted by *Conv* ($k \times l$ @ m), where $k \times l$ is filter size and m is the number of filters. In this study, the max pooling layer is used in the CNN model. The classification stage is composed of several fully-connected layers denoted by *fc(n)*, where n is the number of neurons. The rectified linear units (ReLU) [16] is connected with every convolutional and fully-connected layers, and the dropout [17] with probability 0.6 is used after the fully-connected layers to reduce the over-fitting problem.

To classify the fault degree of ISCr in the battery cell, the proposed CNN model is used and depicted in Fig. 1. The proposed model contains 32 convolutional layers, 8 pooling layers, a fully-connected layer and a softmax layer, denoted by *Softmax*. The max pooling layer is connected after 4 convolutional layers in the CNN model.

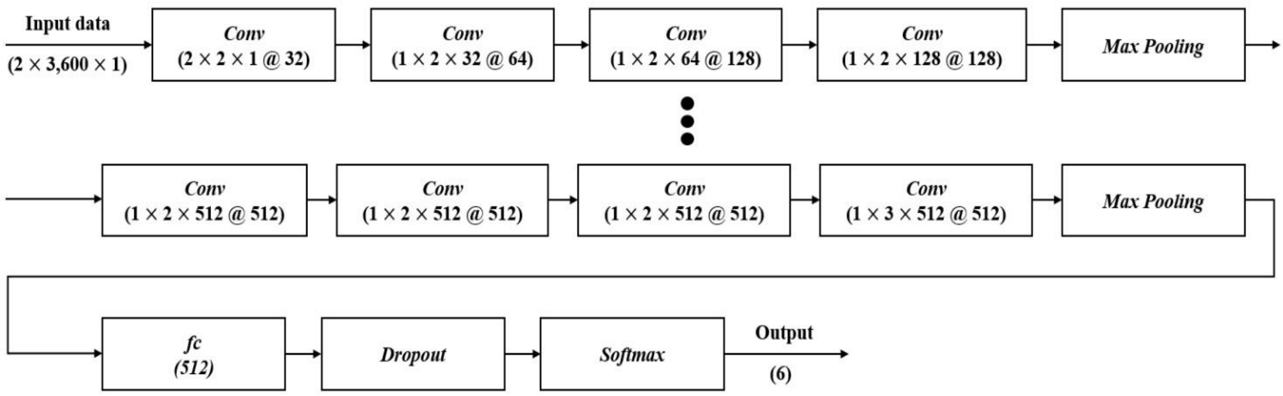

Figure 1. Architecture of proposed CNN model.

B. Preprocessing of Input Data

The equivalent circuit model of the battery cell is shown in Fig. 2, and the R_{ISCr} is connected with the first-order RC model in parallel to represent the ISCr, where the OCV is V_{oc}, internal resistance is R_0, RC network is composed of a resistance R_1 and a capacitor C_1. Due to the ISCr, the load current I_L is divided into two currents; the self-discharge current is I_2 flowing through the R_{ISCr} and the other current I_1 is remainder of the current.

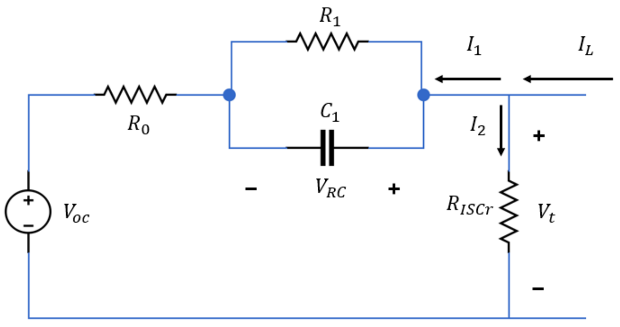

Figure 2. Equivalent circuit model of battery cell with ISCr.

The terminal voltage V_t is represented with (1), where the voltage of the RC network is V_{RC}. To reflect the self-discharge phenomenon caused by the ISCr in the V_t clearly, terms which are related with the I_L having high C-rate in (1) should be removed from the V_t. The OCV for the I_L is eliminated in the V_{oc} necessarily because the first term V_{oc} accounts for a great part of the V_t.

$$V_t = V_{OC} + R_0(I_L - I_2) + V_{RC} \tag{1}$$

When the ISCr occurs in the battery, the SOC of the faulted cell (SOC_f) is represented with the Coulomb counting method [18] in (2), where C_{max} is capacity of the battery, k is sample index and η is the charging and discharging efficiency. The SOC of the normal cell (SOC_n) is equal to $SOC_f(0) + \frac{\eta}{C_{max}}\sum_{n=1}^{k-1} I_L(n)$ in (2), and the SOC_n can be calculated with both the $SOC_f(0)$ and the $I_L(n)$.

$$SOC_f(k) = SOC_f(0) + \frac{\eta}{C_{max}}\sum_{n=1}^{k-1} I_L(n) - \frac{\eta}{C_{max}}\sum_{n=1}^{k-1} I_2(n) \tag{2}$$

To obtain the OCV of the normal cell (OCV_n), the relation between OCV and SOC of the battery is used and shown in Fig. 3. If the relation in a specific range from 100% SOC to 50% SOC is assumed to be linear equation, the function g can describe the relation in (3), where a and b are two coefficients

$$OCV_n(k) = g\big(SOC_n(k)\big) = aSOC_n(k) + b \tag{3}$$

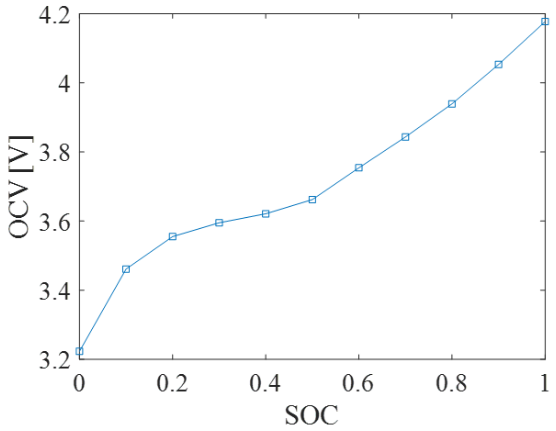

Figure 3. Relation between OCV and SOC.

Subsequently, terminal voltage ($V_{t,pre}$) obtained from the data pre-processing is calculated with (4), and in addition, the R_0I_L is also subtracted from the V_t. In case of normal battery, if the OCV_n is subtracted from the V_t, the $V_{t,pre}$ does not decrease nearly. Therefore, the 80% amount of OCV_n is removed in the V_t. During conducting the data pre-processing in the specific range, the $V_{t,pre}$ and I_L are stored as training and verification data for the CNN until the $V_{t,pre}$ is lower than a certain value. The remainder data of both $V_{t,pre}$ and I_L are defined as 0 after the $V_{t,pre}$ reaches the particular value.

$$V_{t,pre}(k) = V_t(k) - R_0I_L(k) - \big(g\big(SOC_n(k)\big) - b\big)\cdot 0.8 \tag{4}$$

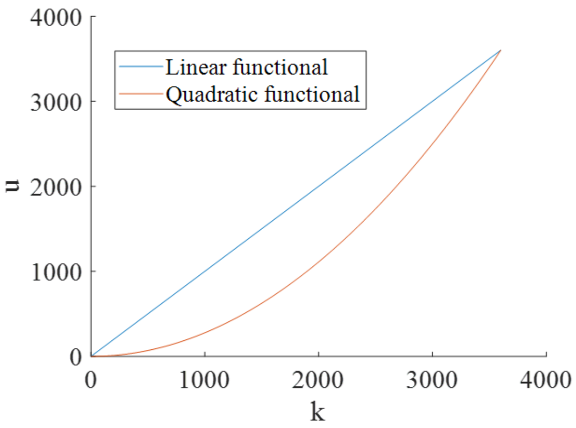

Figure 4. New sample index obtained from quadratic functional.

After obtaining the $V_{t,pre}$ and analysing it, the percentage of zero-padding in the $V_{t,pre}$s for the diverse ISCr cases is large; to overcome this problem, the terminal voltage ($V_{t,sam}$) sampled with a new sample index u is obtained from the quadratic functional h in (5) and Fig. 4. The I_L is also extracted by the same sampling method.

$$u = h(k) \tag{5}$$

$$V_{t,sam}(k) = V_{t,pre}(u)$$

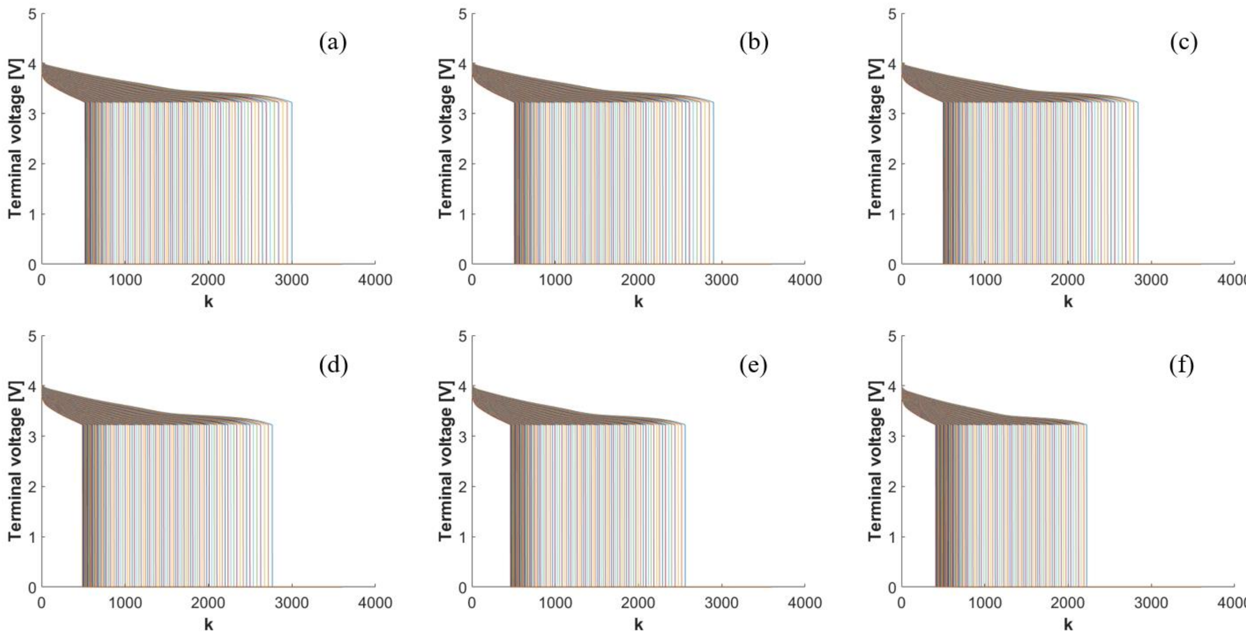

Figure 5. Terminal voltages (V_t) for normal case (a) and various ISCr faults cases; ISCr 50 Ω (b), ISCr 30 Ω (c), ISCr 20 Ω (d), ISCr 10 Ω (e), ISCr 5 Ω (f).

IV. Results and Discussions

A. Results without Data Pre-processing

Fig. 5 shows the V_ts of the battery in the simulation for normal case and diverse ISCr fault cases. For each cases, 1000 constant currents with different C-rates were applied to the battery simulator, and then the 1000 V_ts were obtained. As the magnitude of ISCr resistance was small, the magnitude of self-discharge current was large. Hence, the battery with the small magnitude of ISCr resistance was discharged rapidly. However, due to the high C-rate of constant currents whose magnitude was more larger than that of self-discharge currents, the self-discharge phenomenon was not observed obviously in the data of V_t, resulting in low classification accuracy for both training and verification data in Fig. 6. Mean value of accuracy data with a range from 50th epoch to 99th epoch was determined as a performance index, and the mean values for training and verification data were 42.9%.

B. Results with Data Pre-processing

The $V_{t,sam}$s for normal case and various ISCr fault cases are depicted in Fig. 7. Compared with the V_ts in Fig. 5, by removing the elements related with the constant currents from the V_t in the data pre-processing, the $V_{t,sam}$s reflected the effect of ISCr clearly. Therefore, the classification accuracy of both training and verification data increased significantly in Fig. 8, and the mean values with the range from 50th epoch to 99th epoch were 76.2% for training data and 82.3% for verification data. Learning process with the CNN model was conducted continuously until the epoch was 300, because the accuracy of both data did not converge until the epoch was 100 in Fig. 8. As a result, the accuracy increased gradually and converged after the epoch was 200. In addition, the mean values with the range from 200th epoch to 299th epoch were 95.1% for training data and 96.0% for verification data. Therefore, the ISCr caused in the battery can be detected early by classifying the fault degree of ISCr correctly with the proposed method, and then the battery management system can give enough time to cope with the ISCr.

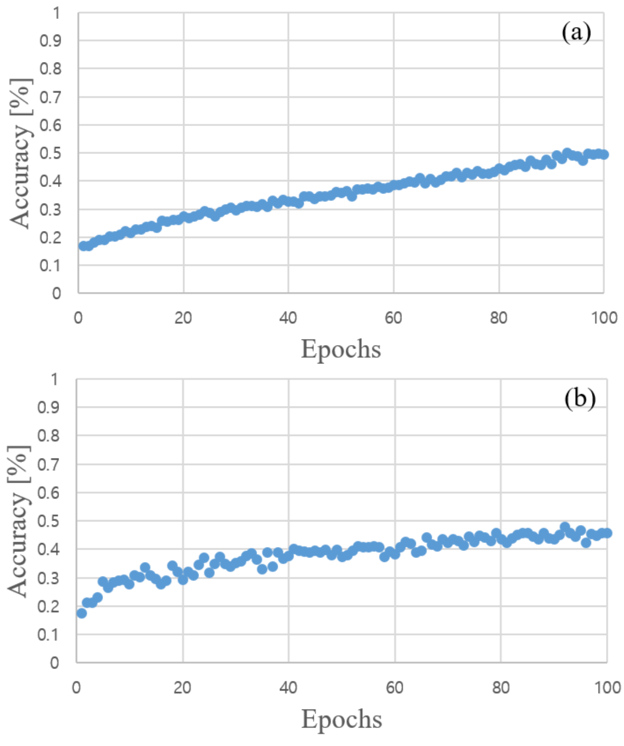

Figure 6. Classification accuracy of training data (a) and verification data (b) with V_t.

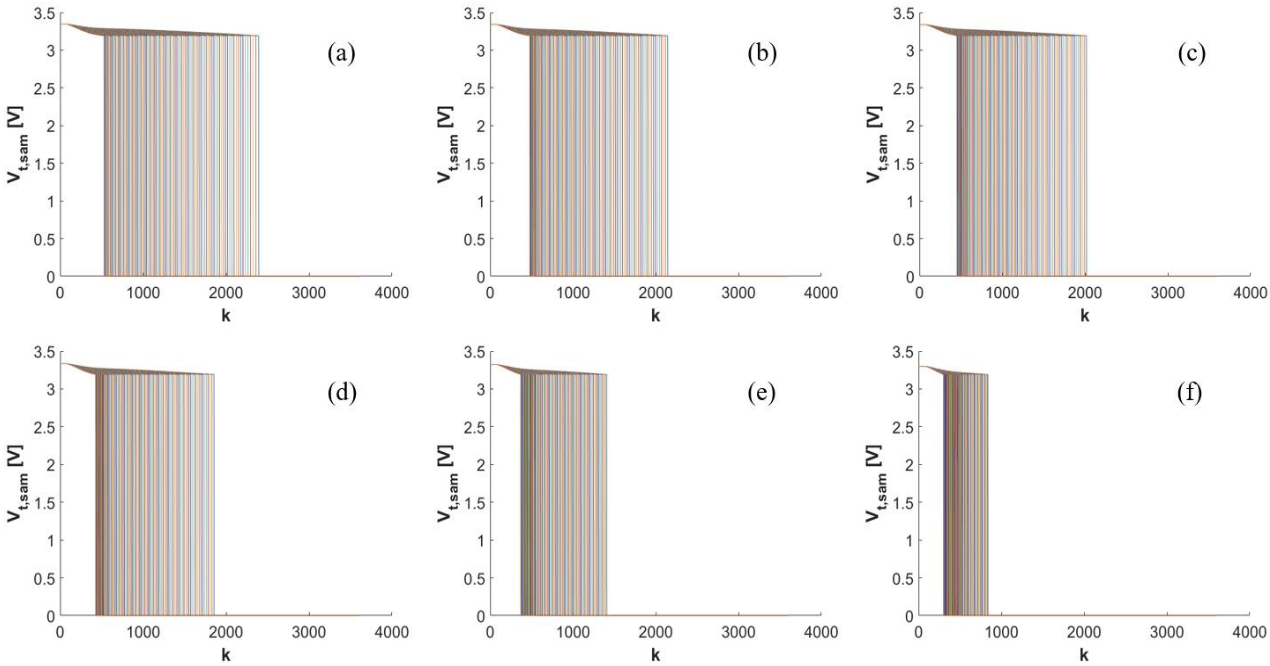

Figure 7. $V_{t,sam}$s for normal case (a) and various ISCr faults cases; ISCr 50 Ω (b), ISCr 30 Ω (c), ISCr 20 Ω (d), ISCr 10 Ω (e), ISCr 5 Ω (f).

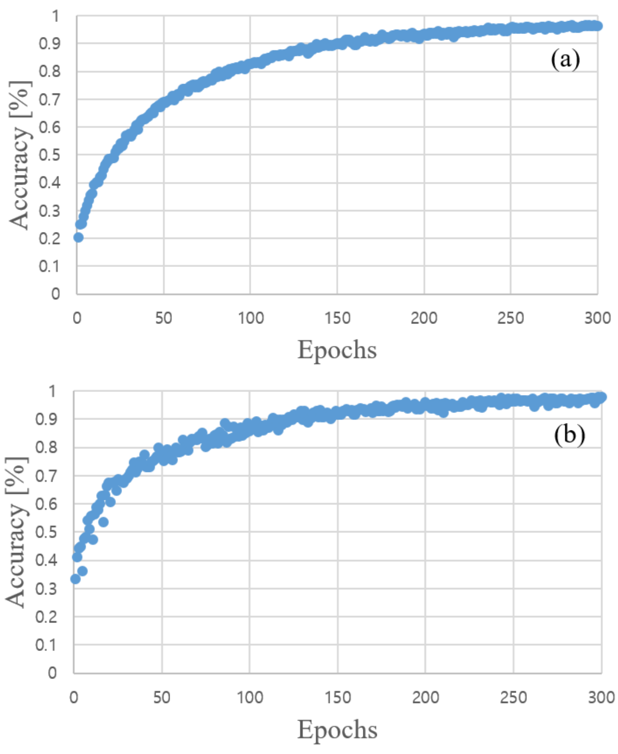

Figure 8. Classification accuracy of training data (a) and verification data (b) with $V_{t,sam}$.

V. CONCLUSION

In this paper, the detection method for the ISCr in the battery by classifying the degree of faults with the CNN algorithm was introduced. When the battery was discharged with the constant currents, it was difficult to estimate the accurate parameters in the equivalent circuit model of battery with ISCr, leading to problem of detection of the ISCr. Therefore, the CNN algorithm was used to develop the learning CNN model for classifying both normal case and various ISCr fault cases. To reflect the self-discharge phenomenon cause by the ISCr obviously, as the data pre-processing, the terms related with the constant currents in the equation for calculating the terminal voltages were removed; this process improved the classification accuracy greatly. The data of terminal voltages and load currents, obtained from the battery simulator, were used to verify the proposed method. The soft ISCr faults with large magnitudes of the ISCr resistance were classified with high accuracy, and then the soft ISCr can be detected by the proposed algorithm correctly.

ACKNOWLEDGMENT

This work was supported by the National Research Foundation of Korea (NRF) grant funded by the Korea government (MSIT), MSIT: Ministry of Science and ICT (2018R1A2B6005522).

REFERENCES

[1] C. Clemente and O. Veneri, "Experimental analysis on the performance of lithium based batteries for road full electric and hybrid vehicles," *Applied Energy*, vol. 136, pp. 921-930, 2014.

[2] H. Chen, *et al.*, "Progress in electrical energy storage system: A critical review," *Progress in Natural Science*, vol. 19, no. 3, pp. 291-312, 2009.

[3] J. M. Tarascon and M. Armand, "Issues and challenges facing rechargeable lithium batteries," *Materials for Sustainable Energy: A Collection of Peer-Reviewed Research and Review Articles from Nature Publishing Group*, pp. 171-179, 2011.

[4] J. M. Kolly, J. Panagiotou, and B. A. Czech, "The investigation of a lithium-ion battery fire onboard a Boeing 787 by the US National Transportation Safety Board," *Safety Research Corporation of America: Dothan, AL, USA*, pp. 1-18, 2013.

[5] M. Gikas and J. Beilinson. (2017). Samsung investigation reveals new details about Note7 battery failures. *Consumer report*. [Online]. Available: https://consumerist.

com/2017/01/22/samsung-investigation-reveals-new-details-about-note7-battery-failures

[6] X. Feng, *et al.*, “Analysis on the fault features for internal short circuit detection using an electrochemical-thermal coupled model,” *Journal of the Electrochemical Society*, vol. 165, no. 2, pp. A155-A167, 2018.

[7] B. Xia, *et al.*, “Multiple cell lithium-ion battery system electric fault online diagnostics,” in *Proc. Transportation Electrification Conference and Expo*, Metro Detroit, 2015.

[8] X. Feng, *et al.*, “Online internal short circuit detection for a large format lithium ion battery,” *Applied Energy*, vol. 161, pp. 168-180, 2016.

[9] M. Seo, T. Goh, G. Koo, M. Park, and S. W. Kim, “Detection of internal short circuit in Li-ion battery by estimating its resistance,” in *Proc. the 4th IIAE International Conference on Intelligent Systems and Image Processing*, Kyoto, 2016.

[10] M. Seo, T. Goh, M. Park, G. Koo, and S. W. Kim, “Detection of internal short circuit in lithium ion battery using model-based switching model method,” *Energies*, vol. 10, no. 1, p. 76, 2017.

[11] L. W. Yao, J. A. Aziz, P. Y. Kong, and N. R. N. Idris, “Modeling of lithium-ion battery using MATLAB/Simulink,” in *Proc. 39th Annual Conference of the IEEE Industrial Electronics Society*, Vienna, 2013, pp. 1729-1734.

[12] B. Y. Liaw, G. Nagasubramanian, R. G. Jungst, and D. H. Doughty, “Modeling of lithium ion cells—A simple equivalent-circuit model approach,” *Solid State Ionics*, vol. 175, pp. 835-839, 2004.

[13] H. He, X. Zhang, R. Xiong, Y. Xu, and H. Guo, “Online model-based estimation of state-of-charge and open-circuit voltage of lithium-ion batteries in electric vehicles,” *Energy*, vol. 39, no. 1, pp. 310-318, 2012.

[14] A. Krizhevsky, I. Sutskever, and G. E. Hinton, “Imagenet classification with deep convolutional neural networks,” *Advances in Neural Information Processing Systems*, pp. 1097-1105, 2012.

[15] W. Zhang, G. Peng, C. Li, Y. Chen, and Z. Zhang, “A new deep learning model for fault diagnosis with good anti-noise and domain adaptation ability on raw vibration signals,” *Sensors*, vol. 17, no. 2, p. 425, 2017.

[16] V. Nair and G. E. Hinton, “Rectified linear units improve restricted boltzmann machines,” in *Proc. the 27th International Conference on Machine Learning*, Haifa, 2010, pp. 807-814.

[17] G. E. Hinton, N. Srivastava, A. Krizhevsky, I. Sutskever, and R. R. Salakhutdinov, “Improving neural networks by preventing co-adaptation of feature detectors,” arXiv preprint arXiv: 1207.0580, 2012.

[18] G. L. Plett, “Extended Kalman filtering for battery management systems of LiPB-based HEV battery packs: Part 3. State and parameter estimation,” *Journal of Power Sources*, vol. 134, no. 2, pp. 277-292, 2004.

Minhwan Seo was born in Deagu, South Korea, in 09 Nov 1991. He received the B.S. degree in electronic engineering in 2015 from Kyungpook National University, Deagu, South Korea and the M.S degree in electrical engineering in 2017 from Pohang University of Science and Technology, Pohang, South Korea, where he has been working the Ph.D. degree in electrical engineering since 2017.

His research interests include fault detection, state estimation and control of lithium-ion battery.

Teadong Goh was born in Tongyeong, South Korea, in 16 Nov 1989. He received the B.S degree in electrical engineering in 2012 from Pohang University of Science and Technology, Pohang, South Korea, where he has been working toward the Ph.D. degree in creative-IT engineering since 2012.

His research interests include system analysis with parameter identification and state estimation of lithium-ion battery.

Minjun Park was born in Deagu, South Korea, in 15 July 1989. He received the B.S. degree in electronic engineering in 2014 from Kyungpook National University, Deagu, South Korea and the M.S degree in electrical engineering in 2016 from Pohang University of Science and Technology, Pohang, South Korea, where he has been working the Ph.D. degree in electrical engineering since 2016.

His research interests include state estimation and remain useful life prediction of lithium-ion battery.

Sang Woo Kim (S’83–M’91) was born in Pyeongtack, South Korea, in 14 Aug 1961. He received the B.S., M.S., and Ph.D. degrees in control and instrumentation engineering from Seoul National University, Seoul, South Korea, in 1983, 1985, and 1990, respectively.

In 1992, he joined Pohang University of Science and Technology, Pohang, South Korea, as an Assistant Professor, where he is currently a Full Professor with the Department of Electrical Engineering. In 1993, he was a Visiting Fellow with the Department of System Engineering, Australian National University, Canberra, Australia. His research interests include optimal control, optimization algorithms, intelligent control, wireless communication and process automation.